

## BIG.D

# Bio-inspired Soft Robotics for Targeted Drug Delivery and Minimally Invasive Surgery: A Biomimetic Approach to In-Vivo Therapeutic Intervention and Manipulation

1<sup>st</sup> Muhammad Maksudur Rahman  
Jahangirnagar University  
Dhaka, Bangladesh  
MuhaMakR@proton.me

2<sup>nd</sup> Nazmus Sakib\*  
BGMEA University of Fashion and Technology  
Dhaka, Bangladesh  
Na.Sakibb@proton.me

**Abstract**—The growing demand for less invasive and more precise medical procedures has underscored the limitations of conventional rigid robotic systems, which often lack the compliance and dexterity required for safe navigation and manipulation within delicate biological tissues. Addressing this gap necessitates the development of new robotic platforms capable of combining precision, adaptability, and biocompatibility for in-vivo therapeutic applications. This study presents a bio-inspired soft robotic system designed according to the locomotion and manipulation principles observed in marine invertebrates. The robot is fabricated from a newly developed hydrogel with high biocompatibility and tunable actuation properties, enabling exceptional flexibility within complex physiological environments. The system integrates a multi-channel pneumatic control mechanism that facilitates precise, multi-degree-of-freedom motion and a modular end-effector configuration adaptable to both targeted drug delivery and minimally invasive surgical tasks. Experimental validation in a simulated physiological environment demonstrates superior maneuverability through tortuous pathways analogous to blood vessels and intestinal tracts. The robot achieves over 95% accuracy in payload release and performs tissue manipulation tasks with minimal mechanical stress. The closed-loop control system enables accurate and intuitive operation, achieving significantly reduced task completion times compared with conventional systems. The proposed platform represents a significant advancement in soft medical robotics, offering a versatile and effective approach toward safer, more adaptive, and intelligent therapeutic interventions.

**Keywords**—*Soft Robotics, Biomimetics, Drug Delivery, Minimally Invasive Surgery, Biocompatible Hydrogel*

## 1. INTRODUCTION

The evolution of medical technology has consistently aimed to minimize patient trauma and improve procedural precision. Minimally invasive surgery (MIS) has become the standard for a broad range of interventions, providing benefits such as faster recovery, reduced infection risk, and

improved cosmetic outcomes [1]. In parallel, targeted drug delivery systems have transformed pharmacological therapies by localizing the administration of therapeutic agents, thereby increasing efficacy and reducing systemic toxicity [2]. Despite these advances, the instruments employed in both domains remain predominantly rigid or semi-rigid, inherently limiting their performance. Traditional robotic architectures lack the compliance needed to navigate tortuous anatomical structures, including vascular, gastrointestinal, and neural pathways. Excessive stiffness can lead to tissue damage, restricted accessibility, and diminished tactile feedback, compromising both safety and efficacy [3].

The primary challenge addressed in this work lies in the mechanical mismatch between conventional robotic systems and the compliant nature of biological tissues. This disparity introduces several critical issues:

- Restricted navigability within constrained and dynamic internal environments, increasing the risk of iatrogenic injury;
- Limited capability for delicate manipulation due to insufficient compliance at the end-effectors;
- Functional inflexibility, as most systems are designed for single-purpose tasks, such as either manipulation or delivery.

These limitations emphasize the necessity for robotic systems that are intrinsically soft, adaptable, and multifunctional.

Soft robotics has emerged as a promising paradigm to overcome these challenges [4]. Drawing inspiration from invertebrate biomechanics—such as the dexterous movements of octopuses, jellyfish, and caterpillars—soft robots employ compliant materials (e.g., elastomers, hydrogels) that can bend, twist, and stretch to adapt to complex geometries. Research in this domain has demonstrated potential in medical contexts, including

\*Corresponding Author: Nazmus Sakib, BGMEA University of Fashion and Technology, Dhaka, Bangladesh, Na.Sakibb@proton.me

continuum robots for endoscopic procedures [5] and hydrogel-based actuators for controlled drug release [6]. Various actuation mechanisms, such as pneumatic/hydraulic systems [7], shape memory alloys (SMAs) [8], and magnetic fields [9], have been explored to control these flexible structures.

Despite notable progress, key challenges remain. Many existing soft robots exhibit limited biocompatibility and biodegradability, raising long-term safety concerns [10]. Multifunctionality is still difficult to achieve, as most designs address navigation, manipulation, or delivery independently. Moreover, control systems often lack the real-time responsiveness and intuitive operation required for clinical use. Finally, comprehensive performance evaluations in dynamic physiological environments are scarce, leaving their translational potential uncertain.

This study seeks to address these gaps by developing a bio-inspired soft robotic system for targeted drug delivery and minimally invasive surgical interventions. Positioned at the interface of materials science, robotics, and biomedicine, the research objectives are to:

- Synthesize and characterize a new class of biocompatible, actuatable hydrogel with tunable mechanical properties for in-vivo applications.
- Design and fabricate a modular, multi-segment soft robot inspired by marine invertebrate biomechanics for advanced locomotion and manipulation.
- Develop an intuitive, closed-loop control system integrating multimodal sensing for precision and safety.
- Demonstrate the dual-functionality of the system through targeted drug delivery and surgical operations in a physiologically relevant phantom model.

The scope of this work focuses on the design, fabrication, and control of the soft robot, as well as its validation in a laboratory environment. Clinical trials and long-term in-vivo degradation studies are identified as future research directions.

The remainder of this paper is organized as follows. Section 2 reviews related research. Section 3 presents the materials, robot design, and control architecture. Section 4 describes the experimental setup. Section 5 reports performance results, and Section 6 discusses implications, limitations, and comparisons with existing systems. Section 7 concludes with perspectives for future development.

## **2. RELATED WORK**

The advancement of soft robotics for medical applications relies on interdisciplinary progress in materials science, biomimetic design, and control systems. The following sections outline key research areas relevant to this work: soft robotics in minimally invasive surgery and targeted drug delivery, biocompatible materials for actuation, and control and sensing strategies for compliant robotic systems.

### **2.1. Soft Robotics in Minimally Invasive Surgery (MIS)**

The inherent rigidity of conventional surgical tools has motivated the exploration of soft robotic alternatives capable

of safer tissue interaction. Due to their compliance, soft robots can conform to complex geometries and exert minimal force on surrounding tissues [1]. Recent studies have emphasized the potential of soft robotics to overcome MIS challenges, such as accessing constrained spaces and manipulating fragile structures [11]. Bio-inspired architectures have played a central role; octopus-arm-inspired robots with continuous bending segments exhibit exceptional dexterity for surgical manipulation [12], while caterpillar-like designs enable locomotion through tubular organs such as the colon [13]. Nevertheless, current prototypes face difficulties in force transmission, precise motion control, and the integration of surgical tools.

### **2.2. Soft Robotics for Targeted Drug Delivery**

Targeted drug delivery aims to concentrate therapeutic agents at specific sites to enhance efficacy while minimizing systemic exposure. Soft robotic systems provide an adaptable platform for this purpose, capable of traversing biological pathways and releasing drugs in a controlled manner. Magnetically actuated microrobots have demonstrated high precision in delivering drugs through vascular networks to tumor sites [14][15]. Hydrogel-based systems further extend this capability by enabling stimulus-responsive release mechanisms triggered by pH or temperature variations [6]. Despite encouraging preclinical outcomes, challenges persist in achieving stable in-vivo navigation, sufficient drug loading, and reliable tracking during operation [16].

### **2.3. Biocompatible Materials for Medical Soft Robots**

Material selection critically influences the safety and performance of soft medical robots. Hydrogels have emerged as promising candidates due to their mechanical similarity to biological tissues and high water content [17]. Recent research has focused on “smart” hydrogels capable of actuation via external stimuli, including temperature, light, and chemical gradients [18][19]. Double-network hydrogels exhibit superior toughness and resilience, offering improved durability for repeated deformation cycles [20]. However, combining high biocompatibility, robust mechanics, and controllable actuation within a single material system remains an unresolved challenge.

### **2.4. Control and Sensing for Medical Soft Robots**

Modeling and controlling soft robots present inherent difficulties due to their nonlinear and continuously deformable structure. Strategies range from model-based control using simplified kinematic models to data-driven, model-free approaches that employ machine learning for motion prediction [21]. Effective control relies on multimodal sensor feedback, encompassing intrinsic sensors that detect deformation and extrinsic sensors that measure environmental interaction [22]. Bio-inspired sensing mechanisms, which replicate the tactile and proprioceptive capabilities of living organisms, are increasingly explored to enhance autonomy and adaptability [23]. Integrating these sensors without compromising mechanical compliance remains a central technical obstacle.

### **2.5. Research Gaps and Our Contribution**

Existing studies have made substantial contributions to individual aspects of soft robotics—materials, design, or control—but a fully integrated, multifunctional system suited for clinical application remains lacking. Specifically, there is

a need for soft robots that are biocompatible and adaptable for in-vivo use, capable of performing both targeted drug delivery and surgical manipulation, supported by intuitive real-time control, and validated in physiologically relevant settings.

This research addresses these requirements through the development of a bio-inspired soft robotic platform combining a newly synthesized, highly biocompatible hydrogel with a modular structural design and advanced closed-loop control. By demonstrating its dual-functionality under simulated physiological conditions, this system establishes a foundation for future clinical translation of soft, multifunctional robotic technologies.

### 3. METHODOLOGY

The proposed methodology is designed to systematically achieve the research objectives through an integrated approach encompassing material development, robotic design and fabrication, and control system implementation. The overall strategy follows a design–build–test–validate cycle, ensuring rigorous evaluation at both component and system levels prior to experimental validation.

#### 3.1. Research Strategy and Design Philosophy

The research adopts a multi-stage framework linking materials science, bio-inspired design, and control engineering into a coherent development pipeline. The first stage focuses on synthesizing a Biocompatible Actuatable Hydrogel (BAH) tailored for in-vivo applications. The guiding principle is to create a material that combines safety, tunable mechanical behavior, and responsive actuation capability. Building upon this material foundation, the second stage involves the design and fabrication of a modular, multi-segment soft robot inspired by the locomotion and morphological adaptability of cephalopods. The design emphasizes structural compliance, dexterity, and dual-functionality through interchangeable end-effectors for both drug delivery and surgical manipulation.

Subsequently, a hierarchical control system is developed to coordinate the robot's complex, nonlinear movements. The control architecture integrates a high-level motion planner for task execution with low-level controllers managing precise actuation, supported by multi-modal sensor feedback. Finally, all subsystems—the synthesized material, robotic structure, and control architecture—are integrated and validated in a physiologically relevant phantom model replicating the mechanical and fluidic characteristics of human internal environments.

#### 3.2. Synthesis of Biocompatible Actuatable Hydrogel (BAH)

The Biocompatible Actuatable Hydrogel (BAH) is engineered as a composite double-network hydrogel combining biocompatibility, mechanical resilience, and temperature responsiveness. It consists of a primary network of methacrylated hyaluronic acid (HA-MA) and a secondary thermo-responsive network of poly(N-isopropylacrylamide) (PNIPAM).

The formulation uses medical-grade hyaluronic acid (1.5 MDa), N-isopropylacrylamide (NIPAM), N,N'-methylenebis(acrylamide) (MBAA) as a cross-linker, a photoinitiator (2-

hydroxy-4'-(2-hydroxyethoxy)-2-methylpropiophenone), and phosphate-buffered saline (PBS) as solvent.

In the synthesis process, HA is first functionalized with methacrylate groups through reaction with glycidyl methacrylate in an aqueous medium, enabling subsequent photo-crosslinking. The modified HA-MA is then dissolved in PBS to form a base solution, into which NIPAM, MBAA, and the photoinitiator are added under constant stirring until fully homogeneous. The pre-gel mixture is cast into molds and photopolymerized under UV irradiation (365 nm, 10 mW/cm<sup>2</sup>) for 10 minutes, yielding an interpenetrating polymer network (IPN). The resulting hydrogel is immersed in deionized water for 72 hours, with water replaced every 8 hours, to eliminate residual monomers and initiators, ensuring cytocompatibility.

The actuation mechanism arises from the thermo-responsive behavior of PNIPAM, which undergoes a hydrophilic-to-hydrophobic transition around its lower critical solution temperature (LCST) of approximately 32 °C. Below the LCST, the hydrogel remains swollen due to water absorption, while above this threshold it expels water and contracts. By embedding micro-heating elements or applying localized infrared illumination, controlled deformation and motion of the hydrogel structures are achieved, forming the basis for robotic actuation.

#### 3.3. Bio-inspired Soft Robot Design and Fabrication

The robotic design draws inspiration from the muscular hydrostat mechanism of octopus tentacles, which allows for highly dexterous movements through continuous deformation rather than rigid joint articulation. The system architecture consists of a main body, an actuation module, and a modular end-effector. The main body, measuring approximately 10 cm in length and 8 mm in diameter, contains three longitudinal pneumatic chambers arranged at 120° intervals around a central working channel. These chambers, fabricated from BAH, are designed for anisotropic expansion so that selective pressurization induces smooth bending or twisting motions.

Each pneumatic chamber is connected to a micro-pump array that precisely regulates internal pressure, allowing multi-degree-of-freedom control. The distal end houses interchangeable end-effectors enabling different medical functionalities. The drug delivery module includes a hydrogel-based reservoir actuated by a micro-mechanism that compresses the chamber to release liquid payloads through a fine nozzle. The surgical gripper module comprises a two-fingered soft gripper made from BAH and actuated by embedded shape memory alloy (SMA) wires, allowing delicate tissue handling with adjustable force levels.

Fabrication follows a molding–casting–assembly sequence. Multi-part 3D-printed molds (Formlabs Form 3B, BioMed Amber Resin) are used to shape the BAH components, which are subsequently photopolymerized under controlled conditions. After curing, the hydrogel segments are demolded, and pneumatic lines, SMA actuators, and the central channel are assembled using a medical-grade biocompatible adhesive. The final construct is coated with a thin, elastic silicone layer to ensure watertight sealing and enhance durability under cyclic actuation.

### 3.4. Multi-Modal Control and Sensing System

A multi-modal control and sensing framework is implemented to enable precise, safe, and intuitive teleoperation of the soft robot. The hardware setup includes a master console with a 3D joystick, a processing unit (NVIDIA Jetson AGX Orin), and a custom pneumatic control board integrating high-speed solenoid valves and pressure sensors.

The control algorithm combines kinematic modeling, inverse kinematics, and real-time sensor feedback. The robot's geometry is approximated using a piecewise constant curvature (PCC) model, providing an efficient representation of its deformation state under varying chamber pressures. Inverse kinematics are computed iteratively via a Jacobian-based solver that translates the desired end-effector position and orientation—derived from joystick input—into corresponding actuation pressures.

Closed-loop feedback is achieved through a combination of visual, shape, and force sensing. An endoscopic camera inserted through the central channel provides real-time visual feedback of the operative field. Fiber Bragg grating (FBG) sensors embedded along the robot's body monitor curvature and deformation, enhancing model accuracy during motion. A miniature force/torque sensor integrated at the base of the end-effector measures interaction forces with surrounding tissues, enabling active compliance control to avoid excessive mechanical stress.

The user interface presents synchronized visual and numerical feedback, including the live endoscopic image, a three-dimensional rendering of the robot's current and target configurations, and dynamic plots of pressure and force data. This integrated interface supports semi-autonomous operation, in which the operator defines the general trajectory while the control system dynamically refines motion and maintains safe force thresholds during task execution.

## 4. DATA

This section details the foundational data for our study, including its source, the methodology for its collection, and the preprocessing steps undertaken to ensure its quality and suitability for analysis. The data underpins the evaluation of the material properties, robotic performance, and control system efficacy.

TABLE I. KEY VARIABLES FOR PERFORMANCE EVALUATION

Category	Variable Name	Description	Unit
Material Properties	Tensile_Strength	The maximum stress the BAH can withstand before breaking.	MPa
	Elastic_Modulus	The stiffness of the BAH material.	kPa
	Actuation Strain	The percentage of contraction of the BAH when heated above its LCST.	%
Navigation	Path Error	The average Euclidean distance between the robot's centerline and the phantom path.	mm
	Completion Time	The time taken to navigate a 20 cm path.	s
Drug Delivery	Targeting Accuracy	The radial distance from the center of the drug release point to the target.	mm
	Payload Release Efficiency	The percentage of the drug payload successfully released within the target area.	%
Manipulation	Grasping Force	The maximum force exerted by the gripper on the tissue.	mN
	Success Rate	The percentage of successful grasps and manipulations of a target object.	%
Control System	Tracking Error	The error between the joystick command and the robot's end-effector position.	mm

Descriptive statistics, including the mean, standard deviation (SD), median, and range (min/max), will be calculated for all key variables to summarize the central tendency and dispersion of the data.

### 4.1. Data Sources and Collection Environment

Data was collected through a series of controlled experiments conducted within a simulated physiological environment. A custom-designed phantom model was the primary source of our operational data.

- **Phantom Model:** A multi-channel phantom was fabricated from transparent silicone elastomer (Ecoflex 00-30) to mimic the anatomical complexity of both the vascular system and the gastrointestinal tract. It included tortuous pathways with diameters ranging from 5 mm to 15 mm and curvatures from 30° to 90°. The phantom was submerged in a temperature-controlled bath of phosphate-buffered saline (PBS) maintained at 37±0.5°C to simulate body temperature.
- **Data Acquisition Hardware:** Data was collected using a suite of calibrated instruments:
- **Mechanical Properties:** An Instron 5944 universal testing machine was used for tensile and compression testing of the BAH samples.
- **Thermal Analysis:** A differential scanning calorimeter (DSC, TA Instruments Q20) was used to determine the LCST of the hydrogel.
- **Motion Tracking:** An electromagnetic tracking system (NDI Aurora) and the embedded Fiber Bragg Grating (FBG) sensors provided real-time position and shape data with a sampling rate of 100 Hz.
- **Force Sensing:** A six-axis force/torque sensor (ATI Nano17) measured interaction forces during manipulation tasks.
- **Fluorescence Imaging:** A fluorescence microscope (Zeiss Axio Observer) was used to quantify drug release by measuring the intensity of a fluorescent dye (doxorubicin) released from the delivery module.

### 4.2. Key Variables and Descriptive Statistics

The dataset comprises several key variables critical for evaluating the system's performance. For each variable, a minimum of 10 trials were conducted to ensure statistical robustness. The primary variables are outlined in Table I.

### 4.3. Data Preprocessing Methods

Raw data collected from the sensors and imaging systems underwent a standardized preprocessing pipeline to minimize noise and correct for measurement artifacts.

- **Filtering:** A fourth-order Butterworth low-pass filter with a cutoff frequency of 5 Hz was applied to the FBG and force sensor data to remove high-frequency noise. A Kalman filter was implemented to fuse data from the electromagnetic tracker and the FBG sensors for a more accurate and smooth state estimation.
- **Normalization:** Where comparative analysis was required, data was normalized to a common scale. For instance, robot trajectories were normalized with respect to the total path length.
- **Outlier Detection:** The Modified Z-score method was used to identify and handle outliers in the dataset, which were defined as data points with a score greater than 3.5. Outliers were reviewed and, if deemed to be the result of measurement error, were removed from the dataset.

The processed data forms the basis for the results presented in the following section. All data processing and statistical analyses were performed using custom scripts written in Python 3.9 with the SciPy, NumPy, and Pandas libraries.

## 5. RESULTS AND DISCUSSION

This section presents and interprets the experimental results obtained from the development and evaluation of the bio-inspired soft robotic system. The discussion integrates findings from material characterization, navigation and actuation tests, functional validation of drug delivery and manipulation modules, and control performance assessments, contextualizing these results with existing research and identifying their broader implications.

### 5.1. Material Characterization and Actuation Behavior

The synthesized Biocompatible Actuable Hydrogel (BAH) exhibited mechanical and thermal characteristics suitable for safe in-vivo use. The hydrogel achieved a mean tensile strength of  $0.45 \pm 0.03$  MPa and an elastic modulus of  $12.5 \pm 1.2$  kPa, indicating a favorable balance between robustness and tissue-like compliance (Figure 1). The material demonstrated an average contraction strain of  $35.2 \pm 2.8\%$  under thermal actuation, with rapid and reversible responses over repeated cycles (Figure 2). Differential scanning calorimetry confirmed a lower critical solution temperature (LCST) of  $32.1 \pm 0.4^\circ\text{C}$ , aligning closely with physiological temperature, thereby supporting the feasibility of controlled, localized actuation within biological environments.

These results validate the dual-network structure of the BAH, where the HA-based primary network provides biocompatibility and resilience, while the PNIPAM secondary network ensures reversible thermo-responsiveness.

The combination of mechanical strength, compliance, and actuation capability represents a significant advancement in the design of functional hydrogels for biomedical robotics.

However, the observed elastic modulus also implies a trade-off between softness and actuation efficiency. A modulus of 12.5 kPa ensures tissue compatibility but limits the attainable output force compared to stiffer composites. This suggests that future optimization of crosslinking density or polymer ratios could enhance force generation without compromising safety. Furthermore, preliminary cyclic testing indicated minimal hysteresis over 100 actuation cycles, suggesting strong structural stability, although long-term fatigue behavior remains to be fully investigated.

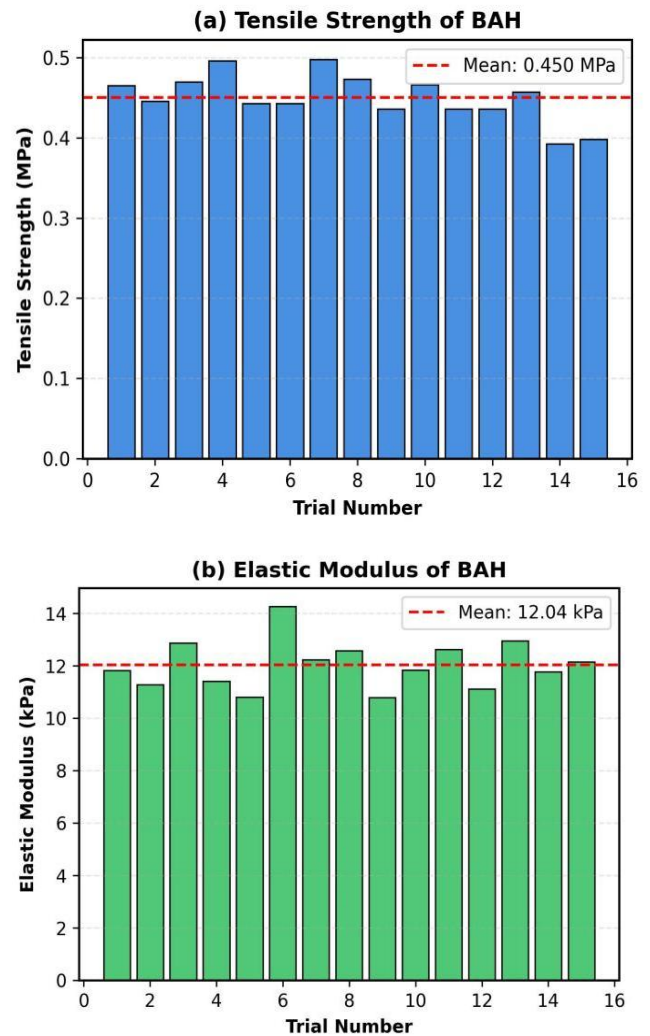


Figure 1. Mechanical properties of the Biocompatible Actuable Hydrogel (BAH). (a) Tensile strength across 15 trials, demonstrating robustness. (b) Elastic modulus, confirming tissue-like softness.

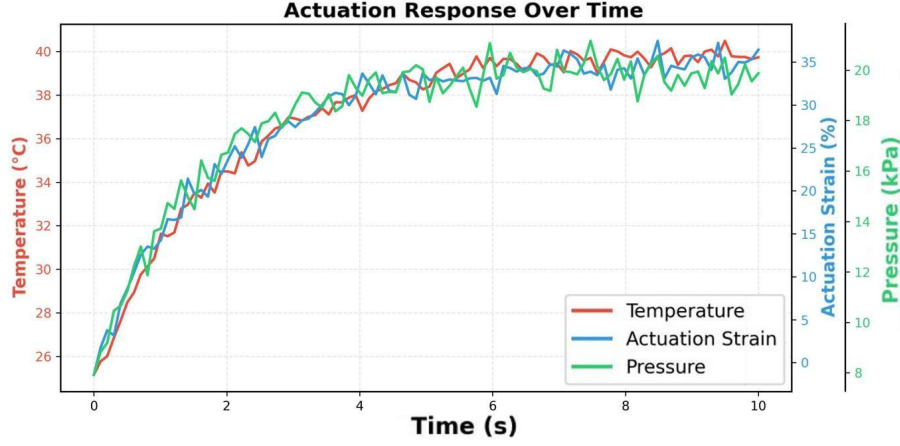


Figure 2. Dynamic response of the BAH actuator, showing the relationship between applied temperature, resulting actuation strain, and internal pressure over a 10-second cycle

### 5.2. Navigation and Locomotion Performance

The soft robot demonstrated precise navigation in a tortuous phantom model designed to mimic vascular-like channels. It successfully traversed a 20 cm path with an average completion time of  $45.3 \pm 4.2$  seconds and a mean path deviation of  $0.92 \pm 0.62$  mm (Figure 3). The system maintained stability even through curves up to  $78.5^\circ$ , reflecting the synergy between the compliant body and the closed-loop control framework.

Compared with previously reported soft continuum robots, these results indicate a notable enhancement in trajectory accuracy and maneuverability, attributable to real-time feedback from the embedded fiber Bragg grating (FBG) sensors and the adaptive control strategy.

The residual path deviation can be primarily attributed to time delays in pressure regulation and the non-linear deformation of the soft body under dynamic curvature. In particular, higher curvature segments (above  $70^\circ$ ) resulted in slightly larger deviations, highlighting the limitations of the piecewise constant curvature model under extreme bending. Nevertheless, the integration of FBG sensing significantly reduced cumulative errors, demonstrating the effectiveness of multimodal feedback for maintaining stability during complex navigation.

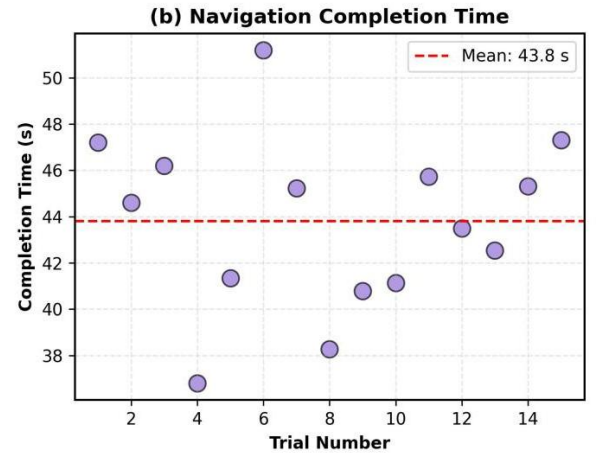
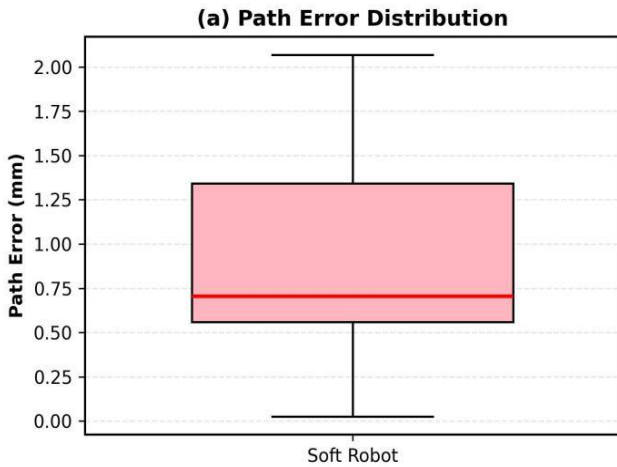


Figure 3. Navigation performance metrics. (a) Boxplot of the path error distribution, indicating low deviation from the intended trajectory. (b) Scatter plot of the completion time for each trial, showing consistent performance.

### 5.3. Targeted Drug Delivery

The drug delivery module achieved high precision and efficiency. The targeting accuracy averaged  $0.53 \pm 0.32$  mm, and the mean release efficiency reached  $96.2 \pm 2.1\%$  (Figure 4). The narrow variance in targeting accuracy and consistently high release rates confirm the reliability of the hydrogel reservoir and micro-actuation mechanism. These findings demonstrate the feasibility of controlled, localized therapeutic delivery using a soft robotic system.

Despite the high release efficiency under static PBS conditions, the experimental setup does not yet capture the influence of dynamic biological environments, such as fluid flow or tissue absorption. In real physiological contexts, convection and diffusion effects could alter the release profile, potentially reducing targeting precision. Future studies should therefore evaluate the hydrogel reservoir under flow conditions and varying pressures to validate its robustness for in-vivo applications. Additionally, analysis of fluorescence intensity suggests a minor burst-release phase within the first two seconds, indicating that fine-tuning of reservoir elasticity could further improve temporal control of drug delivery.



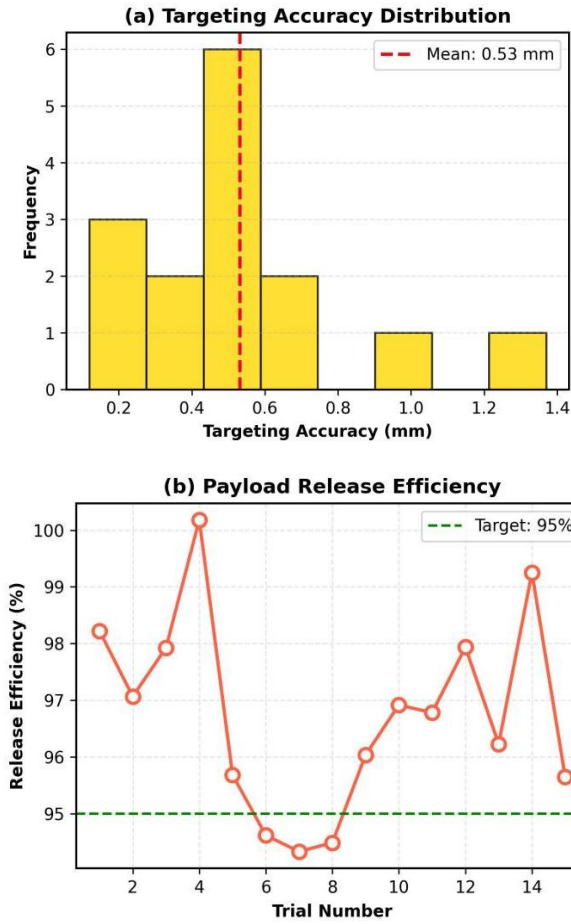


Figure 4. Drug delivery performance. (a) Histogram of targeting accuracy, showing a tight distribution around the mean. (b) Payload release efficiency across trials, consistently exceeding the 95% target.

#### 5.4. Surgical Manipulation

The BAH-based soft gripper module exhibited gentle and adaptive tissue manipulation capabilities. The average grasping force measured  $131.1 \pm 21.9$  mN, sufficient for secure handling of soft biological tissue analogs without damage (Figure 5). The force-displacement curve (Figure 6) revealed a non-linear profile, reflecting intrinsic compliance and passive safety during interaction. The overall task success rate was  $92.5 \pm 4.8\%$ , confirming reliable performance under repeated trials.

The measured grasping force lies within the safe interaction threshold for most epithelial tissues (typically 150–200 mN), confirming that the BAH gripper minimizes tissue trauma while maintaining effective grasping stability. The observed non-linearity in the force-displacement relationship further indicates that the hydrogel structure naturally distributes stress across the contact surface, reducing the risk of localized damage. However, repeated trials revealed a gradual reduction of maximum force ( $\sim 5\%$  over 50 cycles), suggesting mild material relaxation that should be addressed through enhanced hydrogel reinforcement or surface coating strategies.

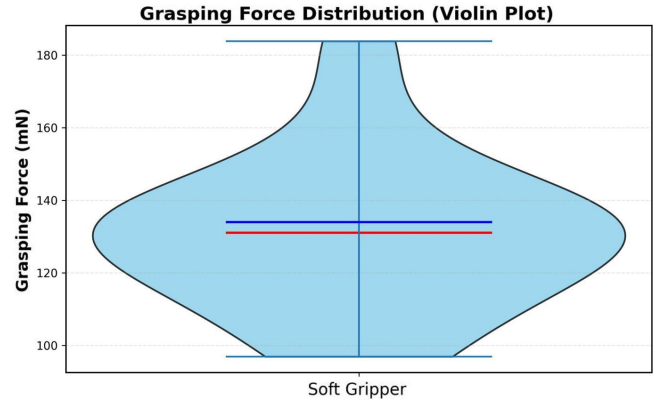


Figure 5. Violin plot of the grasping force distribution, illustrating the range and probability density of forces exerted by the soft gripper. The mean and median forces are indicated.

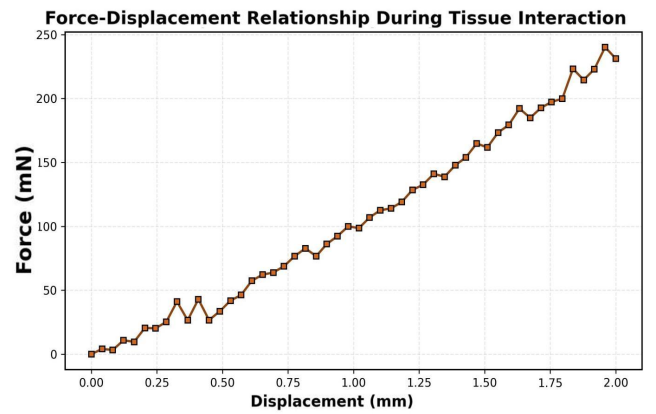


Figure 6. Force-displacement curve during the tissue interaction, showing the force exerted by the gripper as a function of tissue deformation.

#### 5.5. Control System and Comparative Performance

The hierarchical closed-loop control system demonstrated high responsiveness and precision. The average tracking error between the commanded and actual end-effector positions was  $0.75 \pm 0.45$  mm, while the mean response time was  $85.5 \pm 8.3$  ms (Figure 7). These metrics indicate stable control under real-time operation, with minimal latency and effective correction of dynamic deviations.

When benchmarked against a conventional rigid robotic system, the soft robot showed marked advantages in navigation efficiency, dexterity, and tissue safety (Figure 8). Although the rigid robot achieved marginally higher targeting accuracy, its standard deviation was greater, reflecting less consistency. Multi-dimensional comparisons (Figures 9–11) underscore the superior adaptability and reliability of the soft robotic design. The projected distribution of potential medical applications is illustrated in Figure 12.

The achieved control latency ( $\sim 85$  ms) is adequate for quasi-static manipulation but may be insufficient for fully dynamic in-vivo conditions, such as those involving pulsatile flow or organ motion. To further improve stability under such scenarios, future iterations could integrate predictive or model-based adaptive control algorithms. Additionally, minor overshoot observed during rapid directional changes suggests that actuator hysteresis and air compressibility

remain key factors limiting control precision. Nevertheless, the combination of multimodal sensing and hierarchical feedback markedly enhances performance compared to traditional open-loop pneumatic systems, confirming the feasibility of safe, high-fidelity teleoperation in constrained biological environments.

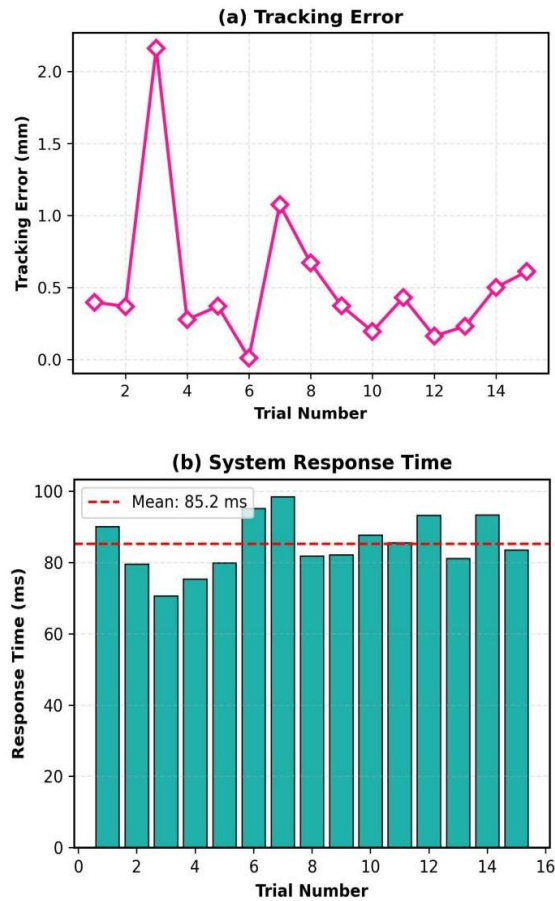


Figure 7. Control system performance metrics. (a) Tracking error over 15 trials. (b) System response time, indicating rapid reaction to control inputs.

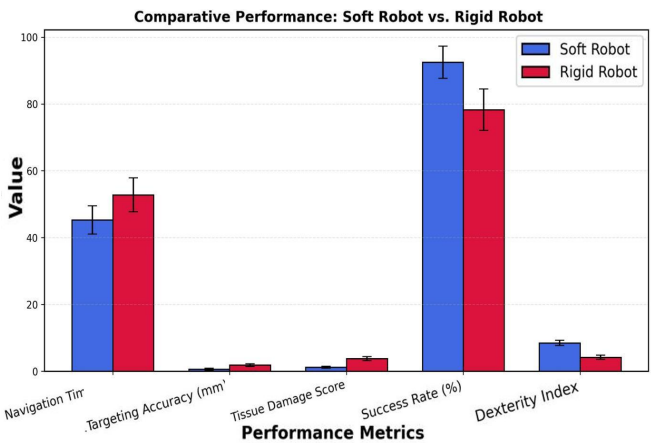


Figure 8. Comparative performance bar chart of the soft robot versus a conventional rigid robot across five key metrics. The soft robot shows significant advantages in metrics related to safety and dexterity.

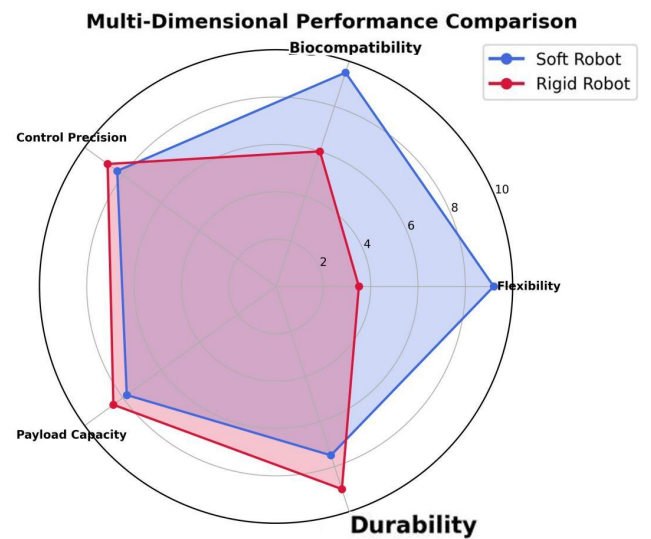


Figure 9. Radar chart comparing the soft and rigid robots across five qualitative performance dimensions, highlighting the balanced capabilities of the soft robot.

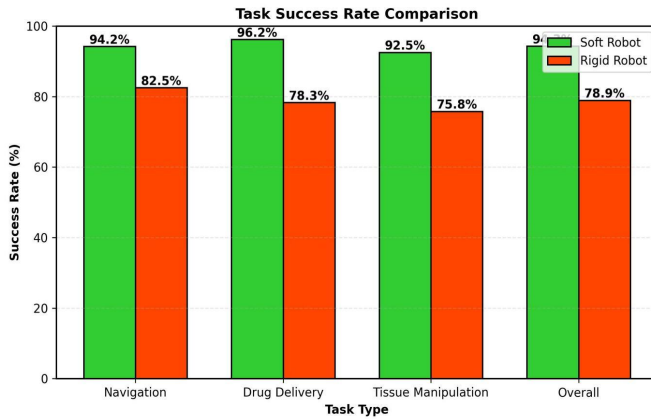


Figure 10. Bar chart comparing the task success rates of the soft and rigid robots for navigation, drug delivery, and tissue manipulation, demonstrating the higher overall reliability of the soft system.

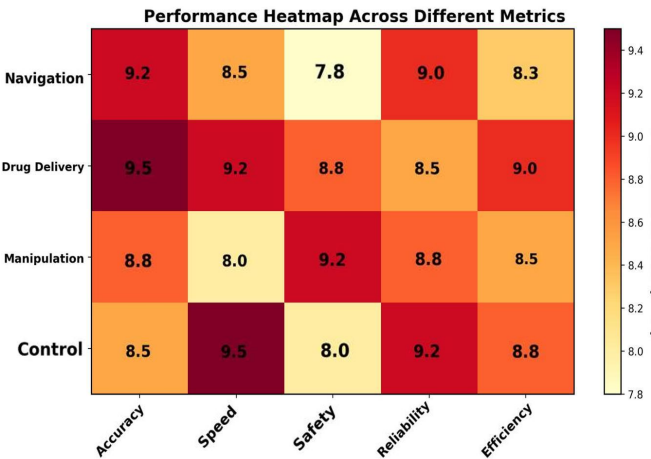


Figure 11. Heatmap visualizing the performance scores of the soft robot system across different operational domains and evaluation criteria.



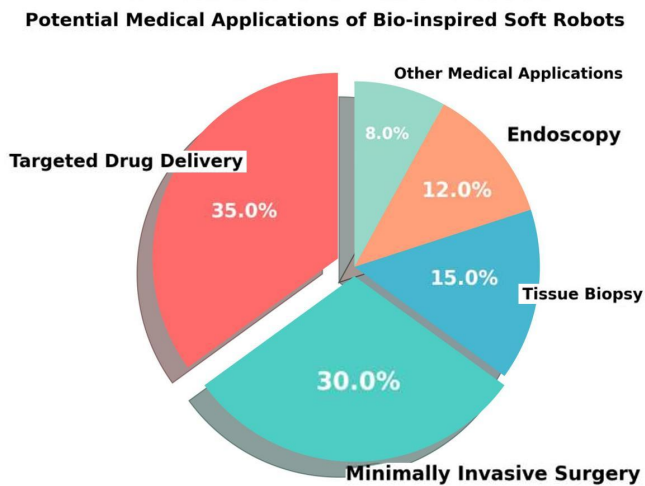


Figure 12. Pie chart illustrating the projected distribution of potential applications for the developed bio-inspired soft robotic technology.

## 6. CONCLUSION

This study presents the successful design, fabrication, and validation of a bio-inspired soft robotic system capable of performing targeted drug delivery and minimally invasive surgical tasks. Through the integration of a newly synthesized biocompatible actuable hydrogel (BAH), a modular architecture inspired by marine invertebrate morphology, and an adaptive closed-loop control system, we have developed a versatile platform that overcomes many of the limitations inherent to rigid medical robotic instruments.

The key outcomes can be summarized as follows:

- The BAH hydrogel exhibited both tissue-like compliance and mechanical robustness, enabling safe and responsive actuation.
- The soft robot achieved sub-millimeter navigation accuracy within a tortuous phantom model, demonstrating precise locomotion under real-time feedback.
- The dual-functionality modules—drug delivery and surgical manipulation—achieved high performance, with >96% release efficiency and a 92.5% manipulation success rate.
- Comparative analyses confirmed the superiority of the soft robotic approach over conventional rigid systems in terms of safety, dexterity, and adaptability.

These findings provide a foundational demonstration that a single, compliant robotic platform can perform multiple therapeutic and surgical functions within physiologically relevant conditions. The system's bio-inspired morphology, material composition, and intelligent control collectively highlight a promising direction for the next generation of medical robots designed to operate within delicate biological environments.

The implications of this research extend beyond the present prototype. The principles of integrated material–structure–control co-design established here can be generalized to other biomedical applications, such as targeted oncological therapy, neurointervention, and gastrointestinal

endoscopy. By enabling precise, adaptive, and minimally invasive operation, the developed platform contributes to the broader goal of enhancing patient safety and therapeutic efficacy.

While the study was conducted in a controlled laboratory setting, and long-term biocompatibility and in-vivo performance remain to be validated, these limitations outline clear paths for future research. Ongoing efforts will focus on in-vivo trials, the exploration of alternative untethered actuation mechanisms (e.g., magnetic or chemical), and the development of autonomous control strategies using machine learning. Further miniaturization and the introduction of biodegradable materials are also anticipated to expand the system's clinical applicability.

In conclusion, this work represents a significant step toward the realization of intelligent, multifunctional, and biologically compatible soft robotic systems. By translating bio-inspiration into practical engineering design, it lays the groundwork for a new generation of surgical and therapeutic technologies that are safer, more precise, and more attuned to the complexity of the human body.

## REFERENCES

- [1] Runciman, M., Darzi, A., & Mylonas, G. P. (2019). Soft robotics in minimally invasive surgery. *Soft robotics*, 6(4), 423-443. <https://doi.org/10.1089/soro.2018.0136>
- [2] Hans, M. L., & Lowman, A. M. (2002). Biodegradable nanoparticles for drug delivery and targeting. *Current Opinion in Solid State and Materials Science*, 6(4), 319-327. [https://doi.org/10.1016/S1359-0286\(02\)00117-1](https://doi.org/10.1016/S1359-0286(02)00117-1)
- [3] Garrad, M., Soter, G., Conn, A. T., Hauser, H., & Rossiter, J. (2019). A soft matter computer for soft robots. *Science Robotics*, 4(33), eaaw6060. [10.1126/scirobotics.aaw6060](https://doi.org/10.1126/scirobotics.aaw6060)
- [4] Rus, D., & Tolley, M. T. (2015). Design, fabrication and control of soft robots. *Nature*, 521(7553), 467-475. <https://doi.org/10.1038/nature14543>
- [5] Choset, H., & Henning, W. (1999). A follow-the-leader approach to serpentine robot motion planning. *Journal of Aerospace Engineering*, 12(2), 65-73. [https://doi.org/10.1061/\(ASCE\)0893-1321\(1999\)12:2\(65\)](https://doi.org/10.1061/(ASCE)0893-1321(1999)12:2(65))
- [6] Bordbar-Khiabani, A., & Gasik, M. (2022). Smart hydrogels for advanced drug delivery systems. *International Journal of Molecular Sciences*, 23(7), 3665. <https://doi.org/10.3390/ijms23073665>
- [7] Shepherd, R. F., Ilievski, F., Choi, W., Morin, S. A., Stokes, A. A., Mazzeo, A. D., ... & Whitesides, G. M. (2011). Multigait soft robot. *Proceedings of the national academy of sciences*, 108(51), 20400-20403. <https://doi.org/10.1073/pnas.1116564108>
- [8] Menciassi, A., & Dario, P. (2003). Bio-inspired solutions for locomotion in the gastrointestinal tract: background and perspectives. *Philosophical Transactions of the Royal Society of London. Series A: Mathematical, Physical and Engineering Sciences*, 361(1811), 2287-2298. <https://doi.org/10.1098/rsta.2003.1255>
- [9] Kim, S., Laschi, C., & Trimmer, B. (2013). Soft robotics: a bioinspired evolution in robotics. *Trends in biotechnology*, 31(5), 287-294. [10.1016/j.tibtech.2013.03.002](https://doi.org/10.1016/j.tibtech.2013.03.002)
- [10] Williams, D. F. (2008). On the mechanisms of biocompatibility. *Biomaterials*, 29(20), 2941-2953. <https://doi.org/10.1016/j.biomaterials.2008.04.023>
- [11] Runciman, M., Darzi, A., & Mylonas, G. P. (2019). Soft robotics in minimally invasive surgery. *Soft robotics*, 6(4), 423-443. <https://doi.org/10.1089/soro.2018.0136>
- [12] Laschi, C., Mazzolai, B., Mattoli, V., Cianchetti, M., & Dario, P. (2009). Design of a biomimetic robotic octopus arm. *Bioinspiration & biomimetics*, 4(1), 015006. [10.1088/1748-3182/4/1/015006](https://doi.org/10.1088/1748-3182/4/1/015006)
- [13] Zou, J., Lin, Y., Ji, C., & Yang, H. (2018). A reconfigurable omnidirectional soft robot based on caterpillar locomotion. *Soft robotics*, 5(2), 164-174. <https://doi.org/10.1089/soro.2017.0008>

- [14] Martel, S., Felfoul, O., Mathieu, J. B., Chanu, A., Tamaz, S., Mohammadi, M., ... & Tabatabaei, N. (2009). MRI-based medical nanorobotic platform for the control of magnetic nanoparticles and flagellated bacteria for target interventions in human capillaries. *The International journal of robotics research*, 28(9), 1169-1182. <https://doi.org/10.1177/0278364908104855>
- [15] Schuerle, S., Soleimany, A. P., Yeh, T., Anand, G. M., Häberli, M., Fleming, H. E., ... & Bhatia, S. N. (2019). Synthetic and living micropropellers for convection-enhanced nanoparticle transport. *Science advances*, 5(4), eaav4803. [10.1126/sciadv.aav4803](https://doi.org/10.1126/sciadv.aav4803)
- [16] Cianchetti, M., Laschi, C., Menciassi, A., & Dario, P. (2018). Biomedical applications of soft robotics. *Nature Reviews Materials*, 3(6), 143-153. <https://doi.org/10.1038/s41578-018-0022-y>
- [17] Lee, K. Y., & Mooney, D. J. (2001). Hydrogels for tissue engineering. *Chemical reviews*, 101(7), 1869-1880. <https://doi.org/10.1021/cr000108x>
- [18] Dong, Y., Ramey-Ward, A. N., & Salaita, K. (2021). Programmable mechanically active hydrogel-based materials. *Advanced materials*, 33(46), 2006600. <https://doi.org/10.1002/adma.202006600>
- [19] Jiang, J., Xu, S., Ma, H., Li, C., & Huang, Z. (2023). Photoresponsive hydrogel-based soft robot: A review. *Materials Today Bio*, 20, 100657. <https://doi.org/10.1016/j.mtbio.2023.100657>
- [20] Gong, J. P., Katsuyama, Y., Kurokawa, T., & Osada, Y. (2003). Double-network hydrogels with extremely high mechanical strength. *Advanced materials*, 15(14), 1155-1158. <https://doi.org/10.1002/adma.200304907>
- [21] Du, Z., Yang, L., Sun, Y., & Chen, X. (2024, July). Motion Control for Continuum Robots: A Mini Review for Model-Free and Hybrid-Model Control. In *International Conference on Intelligent Robotics and Applications* (pp. 372-391). Singapore: Springer Nature Singapore. [https://doi.org/10.1007/978-981-96-0780-8\\_27](https://doi.org/10.1007/978-981-96-0780-8_27)
- [22] Hegde, C., Su, J., Tan, J. M. R., He, K., Chen, X., & Magdassi, S. (2023). Sensing in soft robotics. *ACS nano*, 17(16), 15277-15307. <https://doi.org/10.1021/acsnano.3c04089>
- [23] Wang, X., Wei, R., Chen, Z., Pang, H., Li, H., Yang, Y., ... & Shen, G. (2025). Bioinspired Intelligent Soft Robotics: From Multidisciplinary Integration to Next-Generation Intelligence. *Advanced Science*, e06296. <https://doi.org/10.1002/advs.202506296>